Journal of Clinical Immunology (2019) 39:430–439
https://doi.org/10.1007/s10875-019-00631-6

ORIGINAL ARTICLE

# A Unique Presentation of Infantile-Onset Colitis and Eosinophilic Disease without Recurrent Infections Resulting from a Novel Homozygous *CARMIL2* Variant

Alina Kurolap[1,2] · Orly Eshach Adiv[2,3] · Liza Konnikova[4,5,6] · Lael Werner[7,8] · Claudia Gonzaga-Jauregui[9] · Maya Steinberg[1] · Vanessa Mitsialis[5,6] · Adi Mory[1] · Moran Y. Nunberg[7,8] · Sarah Wall[5] · Ron Shaoul[2,3] · John D. Overton[9] · Regeneron Genetics Center · Alan R. Shuldiner[9] · Yaniv Zohar[2,10] · Tamar Paperna[1] · Scott B. Snapper[5,6,11] · Dror S. Shouval[7,8] · Hagit Baris Feldman[1,2]

Received: 16 September 2018 / Accepted: 14 April 2019 / Published online: 11 May 2019


## Abstract

**Purpose** This study aimed to characterize the clinical phenotype, genetic basis, and consequent immunological phenotype of a boy with severe infantile-onset colitis and eosinophilic gastrointestinal disease, and no evidence of recurrent or severe infections.

**Methods** Trio whole-exome sequencing (WES) was utilized for pathogenic variant discovery. Western blot (WB) and immunohistochemical (IHC) staining were used for protein expression analyses. Immunological workup included in vitro T cell studies, flow cytometry, and CyTOF analysis.

**Results** WES revealed a homozygous variant in the capping protein regulator and myosin 1 linker 2 (*CARMIL2*) gene: c.1590C>A; p.Asn530Lys which co-segregated with the disease in the nuclear family. WB and IHC analyses demonstrated reduced protein levels in patient's cells compared with controls. Moreover, comprehensive immunological workup revealed severely diminished blood-borne regulatory T cell ($T_{reg}$) frequency and impaired in vitro $CD4^+$ T cell proliferation and $T_{reg}$ generation. CyTOF analysis showed significant shifts in the patient's innate and adaptive immune cells compared with healthy controls and ulcerative colitis patients.

**Conclusions** Pathogenic variants in *CARMIL2* have been implicated in an immunodeficiency syndrome characterized by recurrent infections, occasionally with concurrent chronic diarrhea. We show that *CARMIL2*-immunodeficiency is associated with significant alterations in the landscape of immune populations in a patient with prominent gastrointestinal disease. This case provides evidence that *CARMIL2* should be a candidate gene when diagnosing children with very early onset inflammatory and eosinophilic gastrointestinal disorders, even when signs of immunodeficiency are not observed.

Alina Kurolap and Orly Eshach Adiv contributed equally to this work.
Dror S. Shouval and Hagit Baris Feldman contributed equally to this work.

**Electronic supplementary material** The online version of this article (https://doi.org/10.1007/s10875-019-00631-6) contains supplementary material, which is available to authorized users.

✉ Hagit Baris Feldman
hb_feldman@rambam.health.gov.il

[1] The Genetics Institute, Rambam Health Care Campus, Haifa, Israel

[2] The Ruth and Bruce Rappaport Faculty of Medicine, Technion – Israel Institute of Technology, Haifa, Israel

[3] Pediatric Gastroenterology, Rambam Health Care Campus, Haifa, Israel

[4] Devision of Newborn Medicine, Department of Pediatrics, Children's Hospital of Pittsburgh of UPMC, Pittsburgh, PA, USA

[5] Division of Gastroenterology, Hepatology and Nutrition, Boston Children's Hospital, Boston, MA, USA

[6] Harvard Medical School, Boston, MA, USA

[7] Pediatric Gastroenterology Unit, Edmond and Lily Safra Children's Hospital, Sheba Medical Center, Tel Hashomer, Israel

[8] Sackler Faculty of Medicine, Tel Aviv University, Tel Aviv, Israel

[9] Regeneron Genetics Center, Tarrytown, NY, USA

[10] Institute of Pathology, Rambam Health Care Campus, Haifa, Israel

[11] Division of Gastroenterology, Hepatology and Endoscopy, Brigham and Women's Hospital, Boston, MA, USA

**Keywords** *CARMIL2* · *RLTPR* · infantile colitis · very early onset inflammatory bowel disease · immunodeficiency

## Introduction

Infantile-onset inflammatory bowel disease (IBD) refers to a rare group of inflammatory gastrointestinal disorders with onset before the age of 2 years [1, 2]. To date, nearly 100 different monogenic conditions have been described that include gastrointestinal manifestations with an IBD-like phenotype among other systemic features [3]. Considering the intestines are a major lymphoid organ, primary immunodeficiency and immune dysregulation syndromes contribute to more than half of monogenic IBD syndromes. Suspicion for immune-based hereditary IBD disorder is raised by a clinical history of recurrent infections, young age at presentation, severe manifestations, consanguinity, and immunological workup impairments [1, 3].

Recently, several patients with primary immunodeficiency have been described with pathogenic variants in the capping protein regulator and myosin 1 linker 2 (*CARMIL2*), also known as RGD, leucine-rich repeat, tropomodulin, and proline-rich-containing protein (*RLTPR*) [4–7]. *CARMIL2*-immunodeficiency syndrome is characterized by a combined immune defect in T and B cells, as shown by various studies in humans and mice [8]. The limited number of patients reported presented with recurrent infections, mostly of the respiratory system, and cutaneous features, including psoriatic rash, eczema, and skin warts. Chronic diarrhea was observed in some of the patients, though there is limited related phenotypic data [4–7]. We report on a patient with a novel homozygous *CARMIL2* variant, manifesting primarily as infantile-onset colitis and eosinophilic disease.

## Materials and Methods

### Study Participants

The study was approved by the institutional Helsinki committee, and written informed consent was obtained as customary. The studied family included an affected child, both his parents, and a healthy brother.

### Genetic Analysis

"Trio" whole-exome sequencing (WES) was performed in collaboration with the Regeneron Genetics Center (RGC). Protein-coding regions were captured using the IDT xGen capture platform (Integrated DNA Technologies, Coralville, IA, USA) and sequenced on the Illumina HiSeq2500 platform (Illumina, San Diego, CA, USA). We utilized the Genoox data analysis platform Ltd. (Tel Aviv, Israel) and the RGC bioinformatics pipeline for mapping and alignment of the obtained sequence reads to the human genome reference assembly, variant calling and annotation, and subsequent data analysis.

We filtered WES data for rare (defined as variants with a minor allele frequency [MAF] < 0.01 in unaffected controls from population databases, such as gnomAD [9], dbSNP [10], 1000Genomes [11], Greater Middle-East Variome [12], the Rambam Genetics Institute in-house database of 1000 Israeli exomes, and the internal RGC database) coding, protein-altering variants (missense, nonsense, frameshift, and splice site). We investigated all possible disease-causing variants identified by WES, including de novo mutations, X-linked, and compound heterozygous and homozygous variants under a recessive mode of inheritance due to consanguinity between the parents. Pathogenicity of the mutations was assessed by various in silico programs, including SIFT, MutationTaster, and PolyPhen-2 [13–15]. The ConSurf server and SWISS-MODEL were used for protein modeling and variant assessment [16, 17].

The candidate variant in *CARMIL2* was validated and tested for segregation with disease in the healthy brother by Sanger sequencing on an ABI Prism 3500 Genetic Analyzer (Applied Biosystems, Waltham, MA, USA), using 5′-AGAC CACACATTGGGAGAGG-3′ forward and 5′-ACCG GACGTTGAAGTTCCTT-3′ reverse primers.

### RNA Analysis

RNA was extracted from peripheral blood of the patient and a healthy control, using the PureLink RNA Mini kit (Invitrogen, Carlsbad, CA, USA) and reverse transcribed with the High-Capacity cDNA Reverse Transcription Kit (Applied Biosystems), following the manufacturer's protocols. Patient and control cDNA samples and a wild-type gDNA control were analyzed by standard PCR using primers designed to flank over exons 14–21 (forward 5′-CTGAGCCGTCCTAA CGTACT-3′, reverse 5′-ACCCAAAGCAGATGTGTGGT-3′) of *CARMIL2*. The expected cDNA and gDNA sizes were 765 and 1779 bp, respectively. PCR products were subjected to 4% agarose gel electrophoresis with HyperLadder 100 bp (Bioline, London, UK) and Sanger-sequenced to observe the candidate variant effect on splicing.

### Western Blotting

Total protein was extracted from patient and healthy control lymphoblastoid cell lines (LCLs) using RIPA buffer and subjected to SDS-PAGE using standard protocols. The EM-53

anti-CARMIL2 antibody (#11–718, ExBio, Vestec, Czech Republic; 1:500 dilution) was used for protein-of-interest detection, and anti-α-Tubulin (#T9026, Sigma-Aldrich, St. Louis, MO, USA; 1:5000 dilution) was used as a loading control. Results were visualized on ImageQuant LAS 4010 (GE Healthcare, Waukesha, WI, USA) and analyzed using NIH ImageJ software.

### Immunohistochemistry

Formalin-fixed paraffin-embedded 4-μm sections from patient and age- and gender-matched control colonic and esophageal samples were deparaffinized and stained using the EM-53 anti-CARMIL2 antibody (ExBio) diluted at 1:100. Staining was performed on the Ventana Benchmark ULTRA system (Roche Diagnostics, Risch-Rotkreuz, Switzerland). Normal tonsil biopsy was used as a positive control.

### Isolation of Peripheral Blood Mononuclear Cells

Blood was collected in EDTA tubes. Peripheral blood mononuclear cells (PBMCs) were isolated by Ficoll-Paque PLUS (GE Healthcare, Little Chalfont, UK) gradient, according to the manufacturer's instructions.

### In vitro T cell Proliferation

$CD4^+CD45RA^+CD25^-$ naïve T cells were isolated by magnetic-activated cell sorting (MACS) beads (Miltenyi Biotec, Bergisch Gladbach, Germany). Isolation purity was more than 95%. To assess proliferation, we cultured $5 \times 10^5$ mM carboxyfluorescein succinimidyl ester (CFSE)–labeled naïve T cells with soluble αCD3/αCD28-coated beads (ThermoFisher Scientific, Waltham, MA, USA) and IL-2 (100 ng/mL, Peprotech, Rocky Hill, NJ, USA). Proliferation was assessed after 4 days based on CFSE dilution and determined by flow cytometry.

### In vitro $T_{reg}$ Generation

MACS-sorted $CD4^+$ naïve T cells were stimulated with αCD3/αCD28 beads, TGFβ 2 ng/mL (Peprotech), and IL-2 (100 ng/mL) for 4 days. Cells were then fixed, permeabilized, and stained for CD25 and FOXP3.

### Flow Cytometry

Cells were acquired using Navios flow cytometer (Beckman-Coulter, Brea, CA, USA) and analyzed using FlowJo. For FOXP3 staining, fixation/permeabilization kit by eBioscience was used. The following antibodies were used: CD4 clone RPA-T4 (BD Bioscience), CD25 clone 2A3 (BD Bioscience), and FOXP3 clone PCH101 (eBioscience). All flow cytometry experiments were performed in duplicate and a representative image was chosen.

### CyTOF Studies

PBMCs from the *CARMIL2*-immunodeficiency patient, six healthy controls (ages 5–18) and two patients with active ulcerative colitis (UC, ages 18–22), were either stained directly as subsequently described or stimulated for 4 h with 50 ng/mL phorbol myristate acetate (PMA) and 500 ng/mL ionomycin and then stained with a panel of metal-tagged antibodies targeting markers of major immune cell lineages and various cytokines. The samples were run on Helios2 mass cytometer (Fluidigm, San Francisco, CA, USA). FCS files obtained were analyzed with premium Cytobank software and pre-gated on $CD45^+$/viable/single/$DNA^+$ events before initiating the analysis. Normalization beads were used and gated out of the analysis. The data was automatically clustered with Rphenograph and cluster identity was manually labeled based on marker expressed in the individual clusters. The data were also independently reduced on ViSNE plots via Cytobank, once again with manual labeling of cellular populations based on marker expression. Cluster percentage (% of $CD45^+$ viable single events) was computed and plotted for comparison between patient groups using Prism7 software. Cytokine levels were analyzed either by median intensity of the marker within particular clusters or by percent-positive events within that cluster.

## Results

### Case Description

A boy was referred for genetic evaluation at the age of 10 years due to infantile-onset colitis. He was born to healthy parents of Christian Arab descent, who are second-degree cousins (Fig. 1a). The patient presented at age 6 months with chronic bloody diarrhea, accompanied by recurrent fever, aphthous stomatitis, psoriatic rash, severe failure to thrive (FTT), malnutrition, and subsequent physical and motor developmental delays. He did not have recurrent or severe infections that would suggest a primary immunodeficiency. Colonoscopy at the age of 4 years revealed severe active chronic colitis with skip lesions, and hematoxylin and eosin staining demonstrated massive eosinophilic infiltration of the lamina propria of healthy and inflamed colonic mucosa (Fig. 1b). Skin biopsy was consistent with a diagnosis of psoriasis. He was treated with systemic and topical steroids with partial response, and due to FTT and ongoing symptoms, total parenteral nutrition was given for several months; no other medications were used in view of parental objection. His psoriatic rash resolved at 5 years and has not recurred since.

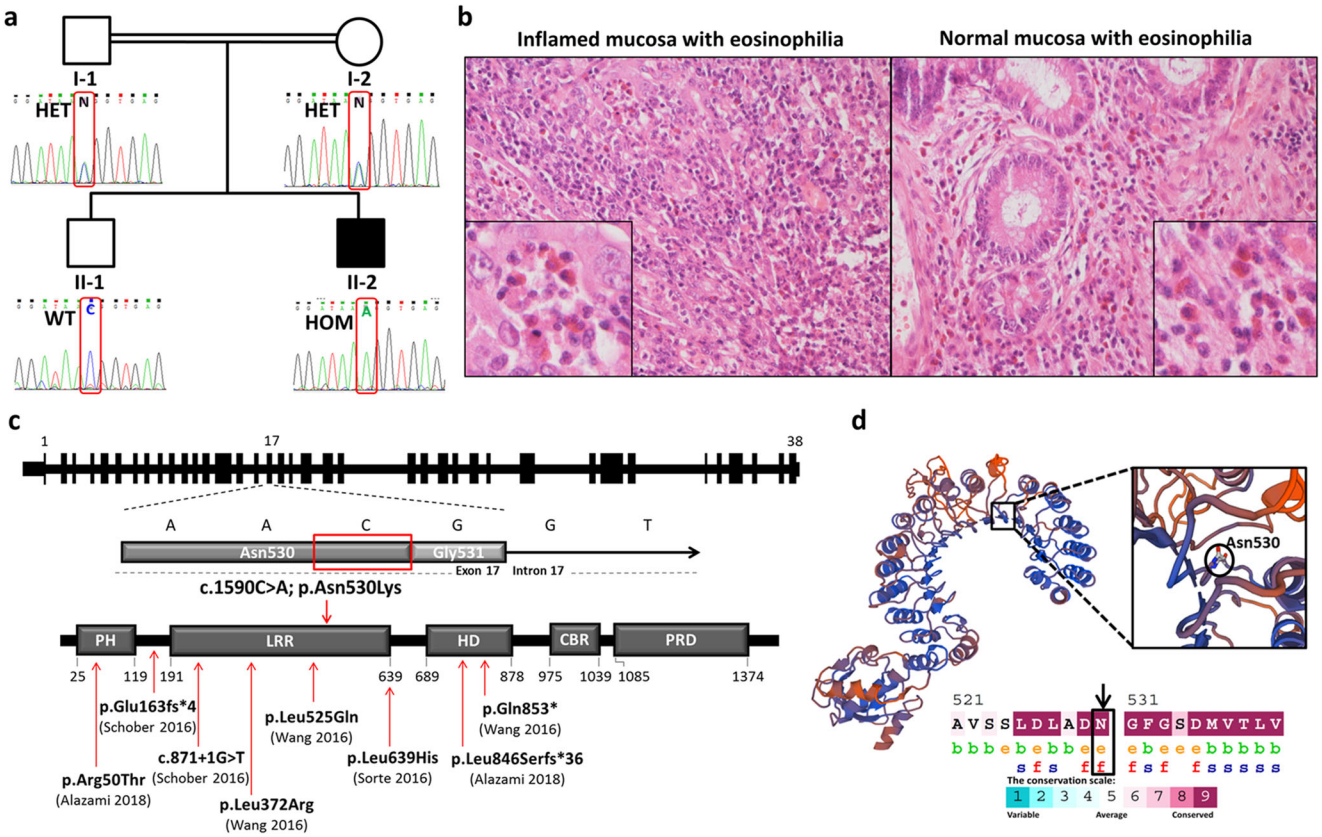


**Fig. 1** A missense variant in *CARMIL2* causes infantile colitis. **a** Pedigree and genotypes of studied family. The c.1590C>A variant segregates as expected for an autosomal recessive disease. **b** Histopathological section of patient's colon tissue, stained with hematoxylin and eosin, revealed skip lesions of healthy and inflamed tissue. Left panel depicts × 40 magnification of inflamed colonic mucosa showing marked increase in eosinophils (in red) in the lamina propria (up to 100 eosinophils per high-power field). Right panel depicts × 40 magnification of healthy colonic mucosa showing granulation tissue with multiple eosinophils (in red). Zoom-in insets are provided for each section to highlight the eosinophilia. **c** Schematic representation of the *CARMIL2* gene (top) and protein (bottom), highlighting the missense variant described in this report (c.1590C>A; p.Asn530Lys) and previously described variations in the gene. The c.1590C>A variant affects the second to the last nucleotide of exon 17, causing an asparagine-to-lysine substitution at position 530 of the protein. PH, pleckstrin homology; LRR, leucine-rich repeat; HD, helical dimerization; CBR, capping protein-binding; PRD, proline-rich domain. **d** 3D homology model of the CARMIL2 LRR region, composed of 16 leucine-rich repeats (modeled by SWISS-MODEL). Asn530 is located within a highly conserved region in LRR 11. It is predicted to be exposed and functional (source: ConSurf server). b, buried; e, exposed; f, functional, s, structural

At 5 years of age, he underwent a sub-total colectomy due to perforation that occurred during routine colonoscopy, leaving him with a protective ileostomy and a rectal pouch. Since then, he suffers from continuous rectal discharge, with repeated rectal biopsies showing eosinophilic proctitis. Over the years, he also developed eosinophilic esophagitis. Amino acid–based formula nutrition combined with topical steroid treatment (oral gel and rectal suppository) was initiated with relatively good results, both clinically and in follow-up esophageal histology. Currently, the boy is thriving properly in terms of height (6th percentile), weight (27th percentile), and cognition. He does not suffer from recurrent infections or exhibits cutaneous findings. His main medical issues revolve around his stoma, rectal discharge, and the fact that he is dependent on a hypoallergenic formula. Eosinophilic infiltration and inflammation are still observed on repeat biopsies.

## Identification of a Novel CARMIL2 Candidate Variant

No pathogenic variants were observed in IBD-related genes, such as *XIAP*, *FOXP3*, and *IL10RA/B* [1]. "Trio" WES analysis identified nine homozygous, three compound heterozygous, four X-linked, and no de novo rare protein-altering variants that passed the filtering criteria described above (Supplementary Table S1). Of these, we prioritized one candidate homozygous novel missense variant, which we considered likely related to the patient's phenotype. The variant occurs in exon 17 of *CARMIL2* (NM_001013838.1): c.1590C>A; p.Asn530Lys (Fig. 1a,c); the amino acid substitution affects the 11th leucine-rich repeat (LRR) domain of the protein (Fig. 1d). The variant has not been reported in general population variant databases or in our internal databases, and it is predicted by all pathogenicity bioinformatic algorithms used. The variant is located 2-bp upstream of

exon's 17 donor splice site and hence we considered possible that it could also affect mRNA splicing (Fig. 1c). However, PCR analysis and Sanger sequencing of the proband's cDNA flanking *CARMIL2* exons 14–21 revealed the expected missense variant of c.1590C>A, without any effect on mRNA splicing (results not shown).

## CARMIL2 Protein Expression

Western blot analysis revealed a marked reduction of 73% in CARMIL2 protein in patient LCLs compared with a healthy control (Fig. 2a).

Immunohistochemical staining for CARMIL2 expression in normal tonsillar tissue (used as positive control) revealed intense staining in endothelial cells, moderate staining in parafollicular lymphocytes, and weak staining in germinal centers (Fig. 2b). The colonic control sample showed positive cytoplasmic staining in lymphocytes, lamina propria plasma cells, crypt epithelium, and endothelium (Fig. 2c), whereas patient samples revealed a lack of staining in lymphocytes and weak, focally positive staining in colonic epithelium and plasma cells (Fig. 2d). No staining was detected in control esophageal squamous epithelium, while intense staining was observed in esophageal immune infiltrates (Supplementary Fig. S1). The patient esophageal sample showed weak staining only in endothelial cells in granulation tissue (Supplementary Fig. S1), compared with intense staining observed in control endothelial cells (Fig. 2b).

## Immunological Analyses

Blood tests at the age of 12 years demonstrated normal immunoglobulin levels. The lymphocyte sub-population assay was overall normal with slightly elevated B cells and decreased $CD4^+$ T cells (Table 1). The level of T cell receptor excision

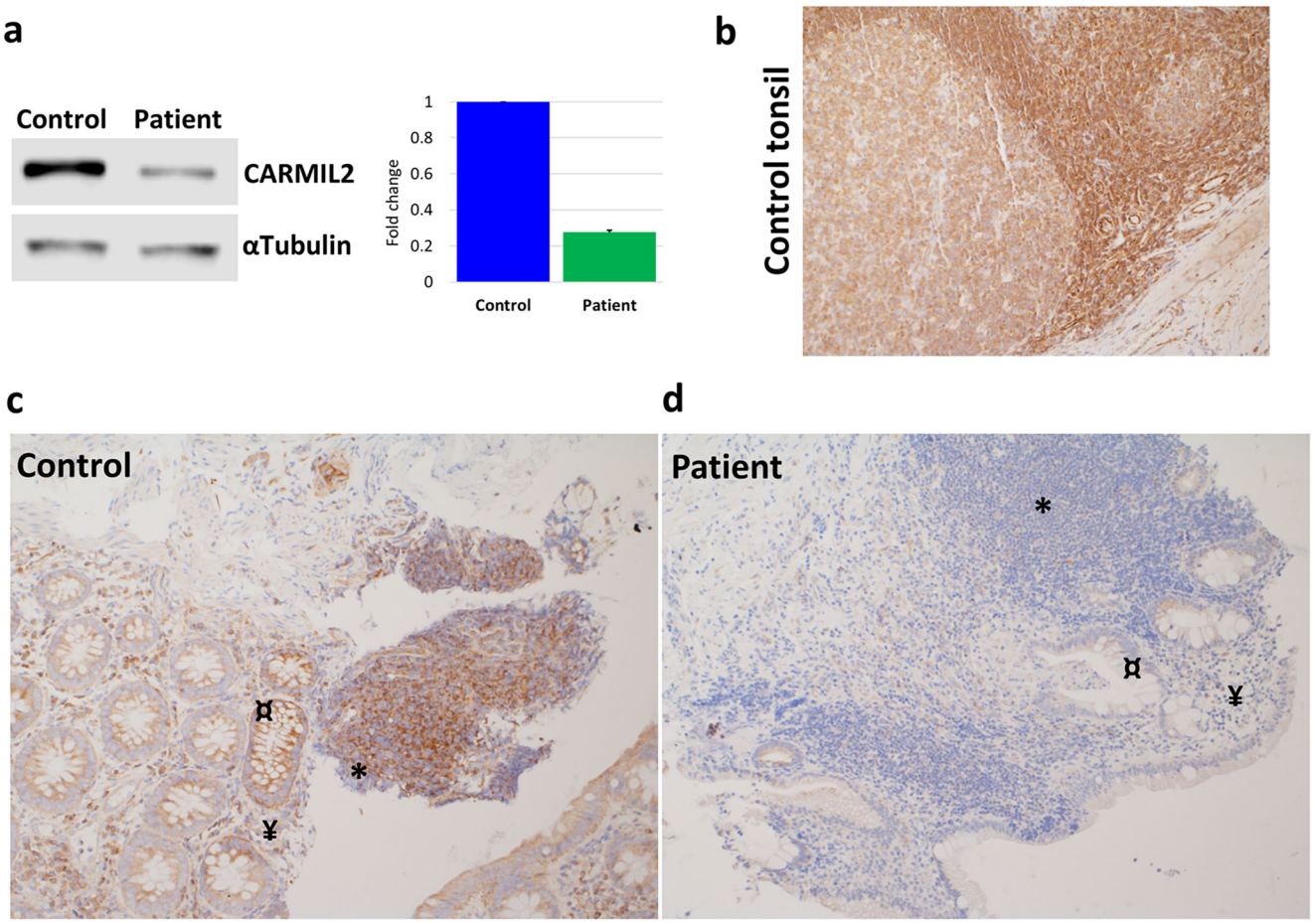


**Fig. 2** CARMIL2 protein expression analyses. **a** Western blot analysis of CARMIL2 reveals 27% protein expression in patient LCLs compared with control LCLs. The figure shows a representative blot from $n = 2$ independent experiments, each performed in duplicate. **b** Normal tonsillar tissue was used as positive control for CARMIL2 immunohistochemical staining, showing a rage of staining intensities in different cell types: intense staining in endothelial cells, moderate staining in parafollicular lymphocytes, and weak staining in germinal centers. **c** Colonic sample from age- and gender-matched control shows positive cytoplasmic staining in lymphocytes (*), lamina propria plasma cells (¥), and crypt epithelium (¤). **d** Patient's colonic sample shows lack of staining in lymphocytes (*) and weak focally positive staining in colonic epithelium (¤) and plasma cells (¥). All immunohistochemical images are depicted at × 20 magnification

**Table 1** Immunological workup of the *CARMIL2*-immunodeficiency patient

| Laboratory | Patient's value | Normal range |
|---|---|---|
| Immunoglobulins | | |
| IgG | 806 mg/dL | 720–1670 mg/dL |
| IgA | 292 mg/dL | 63–304 mg/dL |
| IgM | 180 mg/dL | 49–183 mg/dL |
| Lymphocyte subsets | | |
| WBC | 10,330 cells/$m^3$ | |
| Lymphocytes | 35.8% | |
| $CD3^+$ T cells | 64% | 60–85% |
| $CD4^+$ T cells | *26%* | 36–63% |
| $CD8^+$ T cells | 35% | 15–40% |
| $CD20^+$ B cells | *31%* | 5–25% |
| $CD56^+$ NK cells | 13% | 6–30% |
| T cell studies | | |
| TRECs | 1306 copies/0.5 mg DNA | > 400 copies/0.5 mg DNA |
| TCR v-beta | Polyclonal (normal) | |
| Proliferation | | |
| No mitogen | 249 CPM | 910 CPM |
| PHA 6 mcg/mL | 72,673 CPM | 40,269 CPM |
| PHA 25 mcg/mL | 93,563 CPM | 50,833 CPM |
| CD3 mitogen | *2059 CPM* | 25,200 CPM |

*TREC*, T cell receptor excision circle; *CPM*, counts per minute; *PHA*, phytohemagglutinin
Italicized values reflect abnormal results

circles, a marker of T cell maturation, was normal, as was T cell receptor Vβ repertoire. Previous studies suggested abnormal T cell proliferation among patients with *CARMIL2*-immunodeficiency. T cell proliferation in response to phytohemagglutinin (PHA) was comparable between patient and control, but response to anti-CD3 was reduced in the patient (Table 1), in contrast to previous reports [4, 6]. In more detailed analyses, naïve $CD4^+$ T cells of the patient exhibited diminished proliferation in response to anti-CD3/CD28 and IL-2 stimulation (Fig. 3a). Moreover, in vitro regulatory $CD25^{high}FOXP3^+$ T cell ($T_{regs}$) generation was impaired in the patient cells compared with control (Fig. 3b). A marked decrease in $T_{reg}$ frequency was also observed in peripheral blood of the *CARMIL2*-immunodeficiency patient (Fig. 3c). Overall, our studies are in line with previous findings and suggest a marked impairment in T cell activation in the presence of a mutated CARMIL2.

## CyTOF Analysis of PBMCs

To obtain a more comprehensive overview of the effect of aberrant *CARMIL2* on different immune populations in the blood, we performed CyTOF analysis of PBMCs obtained from the patient and compared the profiles to healthy controls and patients with UC (Fig. 4, Supplementary Fig. S2). There were significant shifts in both innate and adaptive immune cells in the patient compared with controls and UC patients. Our analyses demonstrate that the patient has increased the abundance of effector memory and naïve $CD8^+$ T cells, an increase in naïve $CD4^+$ T cells and transitional B cells ($CD38^+/CD24^+$) compared with controls and patients with UC. In contrast, a significant reduction of $T_{regs}$, memory B cells ($CD27^+$), NK cells, and monocytes was observed in the patient's blood (Fig. 4, Supplementary Fig. S2**)**. We next evaluated cytokine production in response to stimulation with PMA and ionomycin. Overall, cytokine levels were comparable between the groups, including IL-21, IL-22, IL-17, TNF-α, and IL1β (data not shown). However, interferon-γ (IFN-γ) production in the *CARMIL2*-immunodeficiency patient was increased compared with controls in several immune subsets, particularly activated $CD8^+$ T cells (Fig. 5).

## Discussion

We describe a patient with infantile-onset colitis, who was found to harbor a homozygous missense variant in *CARMIL2* (p.Asn530Lys). The previously described immunodeficiency syndrome caused by *CARMIL2* mutations in 11 unrelated families consists predominantly of recurrent infections and cutaneous features; only six of the 21 published patients were reported to have chronic diarrhea, among the other symptoms, and only one patient was described with

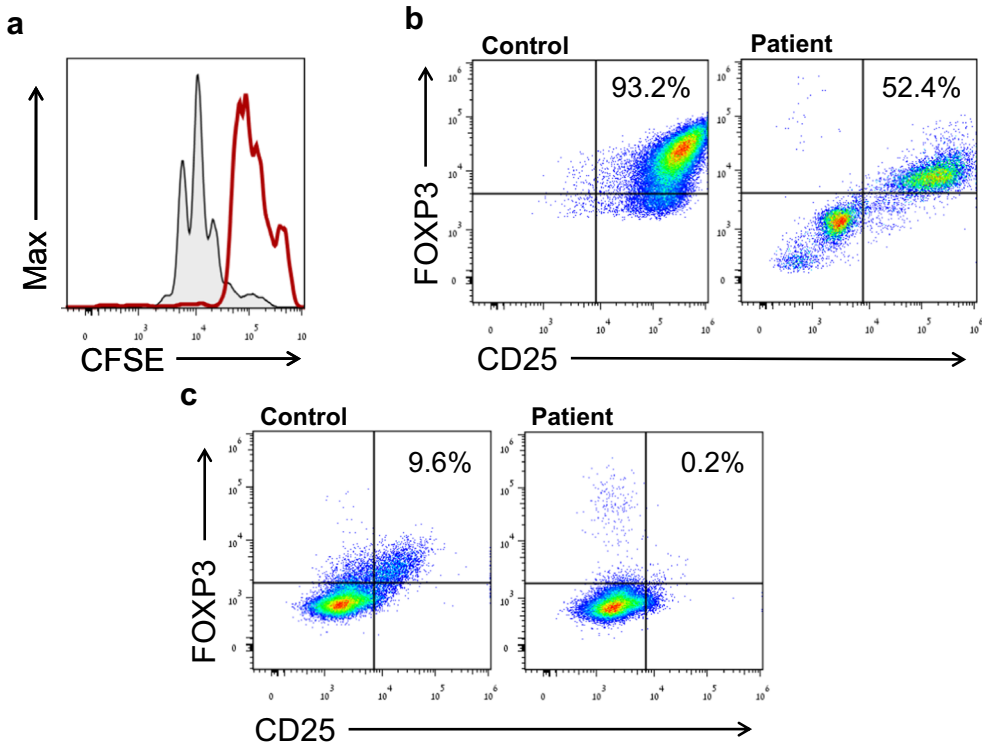


**Fig. 3** Impaired T cell proliferation and Treg generation in *CARMIL2*-immunodeficiency. **a** FACS plot ($n = 1$) showing decreased T cell proliferation of naïve $CD4^+$ T cells of the *CARMIL2*-immunodeficiency patient (red) compared with healthy control (gray). In these studies, each peak going from the right to left corresponds to division of the cells, leading to dilution of the CFSE. **b** In vitro $T_{reg}$ generation assay ($n = 1$) demonstrating diminished production of $FOXP3^+$ T cells from naïve T cells of the patient, under polarizing conditions. **c** $T_{reg}$ frequency in peripheral blood in the patient is reduced, compared with control, as measured by FACS ($n = 1$)

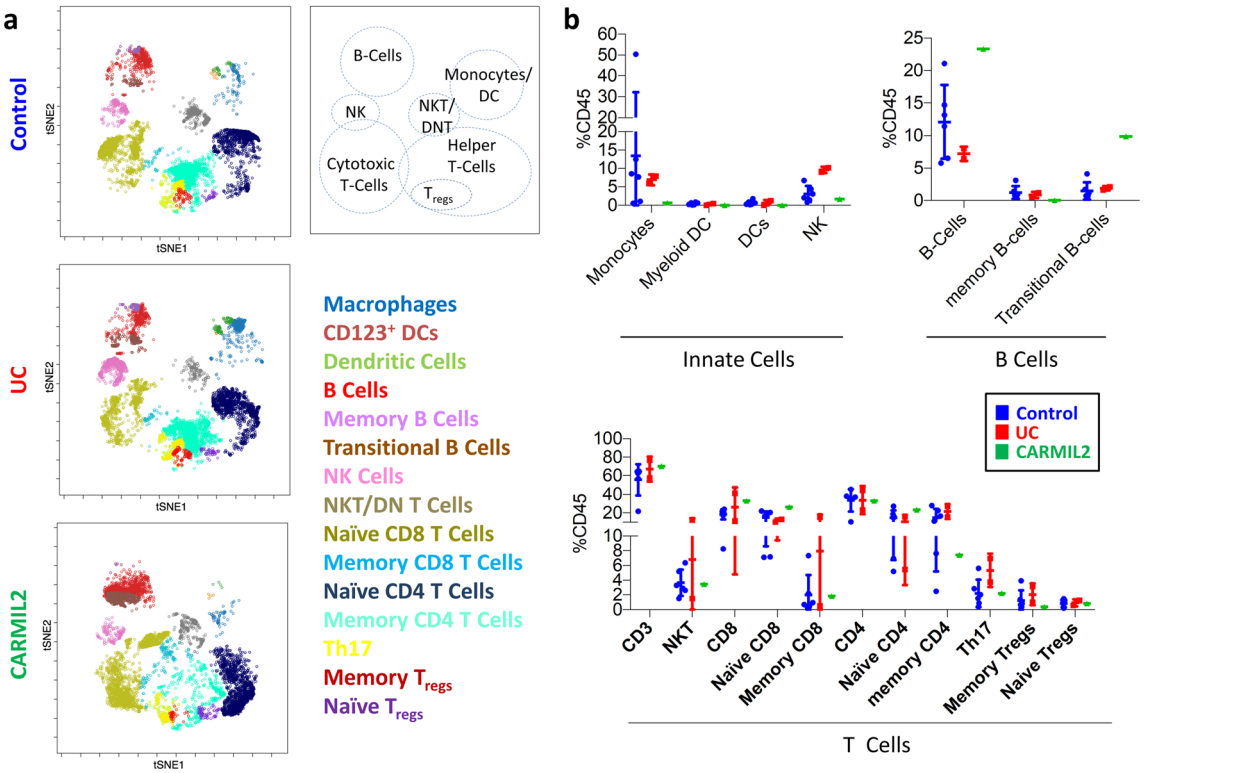


**Fig. 4** Peripheral blood immune alterations in *CARMIL2*-immunodeficiency patient. CyTOF ($n = 1$) was completed on PBMCs from controls ($n = 6$), patients with UC ($n = 2$), and the patient with *CARMIL2* mutation. **a** Representative viSNE plots of PBMCs obtained from the studied patients, followed by cumulative data (**b**) (NK-natural killer cells, $T_{regs}$-regulator T cells, MP-macrophages, nTh-naïve CD4 T cells, nB-naïve B cells, tB-transitional B cells, nTC-naïve CD8 T cells, E.M.Tc-effector memory CD8 T cells, EM-effector memory, DC-dendritic cells, DN-double negative, ILC-innate lymphoid cells)

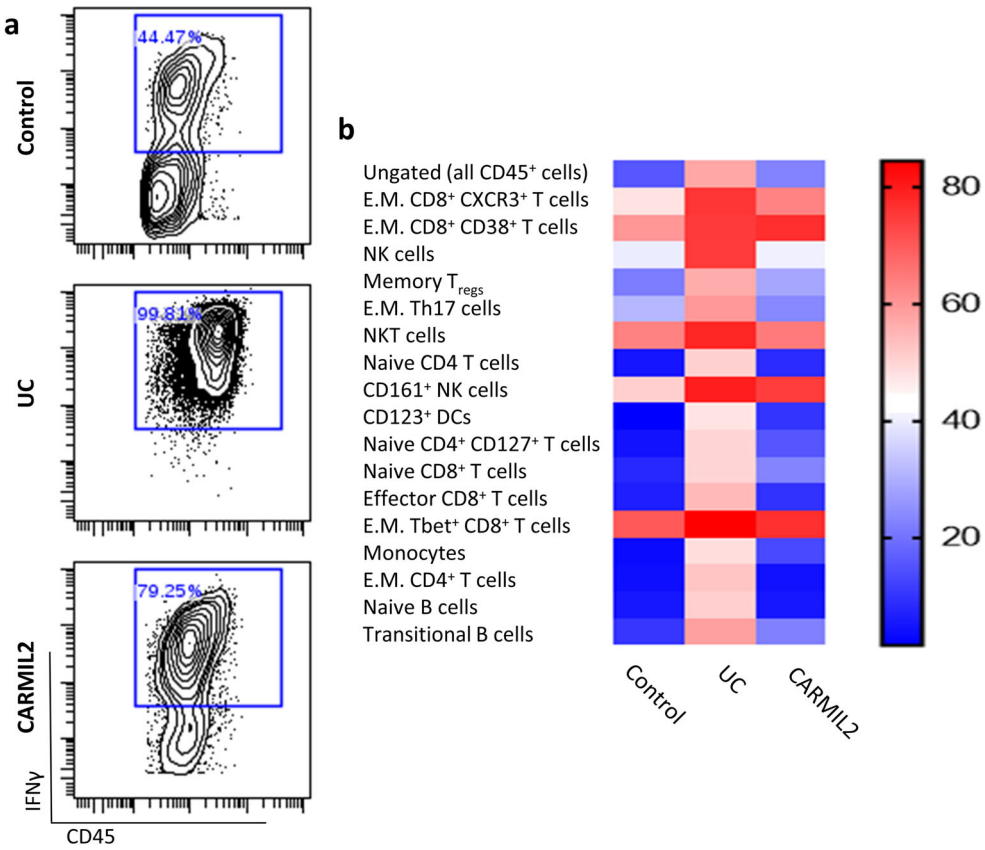


**Fig. 5** IFN-γ production in *CARMIL2*-immunodeficiency. **a** Representative 2D CyTOF plot ($n = 1$) of IFN-γ production by effector memory T cells (CCR7$^-$/CD45RA$^-$). **b** Heat map of IFN-γ production in the clusters generated through automatic clustering of controls ($n = 3$), patients with UC ($n = 2$), and patients with *CARMIL2*-immunodeficiency ($n = 1$)

eosinophilic esophagitis [4–7]. A susceptibility to EBV-related smooth muscle tumors and leiomyosarcoma was observed in some *CARMIL2* patients [4, 5] and required comprehensive follow-up.

Although the patient we describe here presented with a psoriatic rash at an early age as consistent with the other reports, it resolved and did not recur. In addition, he did not suffer from significant respiratory illnesses and chronic viral infections, as often observed in patients with immunodeficiency disorders. Since colitis was the predominant feature of the boy's ailment, he was regarded as an IBD patient and managed accordingly.

Tissue eosinophilia in colonic biopsies is commonly seen in UC, and some studies have shown a negative correlation between the degree of eosinophilia and clinical outcomes [18, 19]. However, significant tissue eosinophilia is also a characteristic of several primary immunodeficiencies that are also associated with monogenic IBDs, such as IPEX syndrome (resulting from *FOXP3* mutations) [20] and occasionally chronic granulomatous disease (resulting from *CYBB*, *CYBA*, *NCF1*, *NCF2*, and *NCF4* mutations) [21]. Our patient, as well as those reported in the literature, exhibited severely diminished $T_{regs}$, similar to IPEX patients. Thus, *CARMIL2*-immunodeficiency should be added to the growing list of IPEX-like diseases, which, beside *FOXP3*, [20] also include mutations in *IL2RA* [22], *MALT1* [23], *STAT1* [24], *CTLA4* [25], *DOCK8* [26], and *LRBA* [27]. Interestingly, despite a lack of $T_{regs}$ in our patient, no additional autoimmune features were noted.

T cell activation and subsequent signal transduction require co-stimulation of CD28. CARMIL2 was found essential for this co-stimulation process by linking CD28 with CARD11 (CARMA1) and activation of the NF-kB pathway [8, 28]. The human *CARMIL2*-immunodeficiency syndrome recapitulates the findings in mouse models, as demonstrated by the immunological workup in the patient described here and in previous studies. Studies in other patients showed global T cell immunity impairment, with poor Th1 and Th17 differentiation and cytokine production, as well as abnormal activation of the NF-kB pathway [4, 6, 8]. While in mice the immune defects could be attributed to T cell dysfunction alone, in humans, the cellular defect appears to overlap both the T and B cells, leading to a combined immunodeficiency (CID) syndrome [6, 8]. Moreover, our CyTOF analysis provides a comprehensive overview of immune cell architecture, showing alterations in the frequency of various other populations, including monocytes and NK cells. The IFN-γ expression was upregulated by different effector cells and might have an important role in mediating the inflammatory response.

CARMIL2 contains five major domains (N- to C-terminal): pleckstrin homology (PH), LRR, helical dimerization (HD), capping protein-binding (CBR), and proline-rich domain

(PRD) (Fig. 1c). The PH, LRR, and PRD have been previously demonstrated to play part in CD28 co-stimulation; therefore, impeding these regions leads to defects in T cell activation, as observed in patients with *CARMIL2* pathogenic variants, including the patient described here [4–6, 8]. The LRR domain of CARMIL2 comprises 16 repeats of the canonical highly conserved LxxLxLxxN/CxL sequence, in which "L" corresponds with leucine, isoleucine, valine, or phenylalanine and "N/C" with asparagine, threonine, serine, or cysteine [29]. The amino acid substitution p.Asn530Lys affects the highly conserved asparagine (N) in position 9 of the 11th LRR sequence (Fig. 1d); the alteration between the polar uncharged asparagine to a positively charged lysine, which also has a larger side-chain, at this position may possibly affect the α/β horseshoe/loop structure of this domain, thus changing its affinity and interaction with other proteins, such as CARMA1 [8, 29]. The outcome from this amino acid substitution is decreased by 73% in protein expression in patient cells compared with a healthy control, highlighting its pathogenicity (Fig. 2a). These findings are similar to a different variant in the same LRR repeat (p.Leu525Gln), which was previously described in a patient of Turkish descent, without reported diarrhea, and shown to cause 65% decrease in protein expression [6]. Interestingly, immunohistochemical analysis of control colonic and esophageal tissues shows expected high CARMIL2 expression in immune cells (lymphocytes and plasma cells), as well as high expression in endothelial cells and moderate expression in colonic epithelial tissue (Fig. 2c, Supplementary Fig. S1). These appear markedly reduced in the patient with mutated CARMIL2, i.e., no expression in colonic and esophageal immune cells and very mild expression in colonic epithelium and in endothelial cells in both tissues (Fig. 2d, Supplementary Fig. S1). These findings may explain the immunological gastrointestinal dysregulation and the clinical phenotype observed in this patient's colon and esophagus. The observation of CARMIL2 expression in colonic epithelial and endothelial cells warrants further study of the role of CARMIL2 in the gut.

Overall, the phenotypical differences between the *CARMIL2*-immunodeficiency patients reported to date emphasize the heterogeneity of clinical symptoms within the same genetic disease and occasionally even in patients with the same genetic variant. One of the X-linked variants observed in the patient's WES, *CYSLTR1* (NM_001282186.1): c.68A>G; p.Asn23Ser may have a modulating effect on his pronounced eosinophilic gastrointestinal disease. *CYSLTR1* encodes a G protein–coupled receptor for cysteinyl leukotrienes and has been previously associated with asthma and eosinophil migration [30]. However, the predicted effects of this variant are not strong (Table S1), and further evaluation is required to assess a possible effect on receptor activity. While the patient did have occasional eosinophilia on blood counts, his blood eosinophil levels are mostly normal and he does not have symptoms consistent with asthma.

In summary, we describe a patient with infantile-onset colitis that harbors a novel homozygous missense *CARMIL2* variant, highlighting the importance of a wide differential diagnosis in patients that present with presumably isolated colitis. The $T_{reg}$ signaling defects observed in this patient support this diagnosis. Diagnosing *CARMIL2*-immunodeficiency in this patient has important clinical implications, requiring a multidisciplinary overview of gastroenterology and immunology experts in patient management.

**Acknowledgments** We thank the patient and his family for participating in this study.

**Funding** D.S.S. is supported by the Israel Science Foundation and Jeffrey Modell Foundation grants. S.B.S. is supported by NIH grants HL59561, DK034854, and AI50950; the Helmsley Charitable Trust; and the Wolpow Family Chair in IBD Treatment and Research.

## Compliance with Ethical Standards

The study was approved by the institutional Helsinki committee, and written informed consent was obtained as customary.

**Conflict of Interest** The authors declare that they have no conflict of interest.

## References

1. Uhlig HH, Schwerd T, Koletzko S, Shah N, Kammermeier J, Elkadri A, et al. The diagnostic approach to monogenic very early onset inflammatory bowel disease. Gastroenterology. 2014;147:990–1007.
2. Kammermeier J, Dziubak R, Pescarin M, Drury S, Godwin H, Reeve K, et al. Phenotypic and genotypic characterisation of inflammatory bowel disease presenting before the age of two years. J Crohn's Colitis. 2017;11:60–9.
3. Uhlig HH, Schwerd T. From genes to mechanisms: the expanding spectrum of monogenic disorders associated with inflammatory bowel disease. Inflamm Bowel Dis. 2016;22:202–12.
4. Schober T, Magg T, Laschinger M, Rohlfs M, Linhares ND, Puchalka J, et al. A human immunodeficiency syndrome caused by mutations in CARMIL2. Nat Commun. 2017;8:14209.
5. Sorte HS, Osnes LT, Fevang B, Aukrust P, Erichsen HC, Backe PH, et al. A potential founder variant in CARMIL2/RLTPR in three Norwegian families with warts, molluscum contagiosum, and T-cell dysfunction. Mol Genet genomic Med. 2016;4:604–16.
6. Wang Y, Ma CS, Ling Y, Bousfiha A, Camcioglu Y, Jacquot S, et al. Dual T cell– and B cell–intrinsic deficiency in humans with biallelic RLTPR mutations. J Exp Med. 2016;213:2413–35.
7. Alazami AM, Al-Helale M, Alhissi S, Al-Saud B, Alajlan H, Monies D, et al. Novel CARMIL2 mutations in patients with variable clinical dermatitis, infections, and combined immunodeficiency. Front Immunol. 2018;9:203.
8. Roncagalli R, Cucchetti M, Jarmuzynski N, Grégoire C, Bergot E, Audebert S, et al. The scaffolding function of the RLTPR protein explains its essential role for CD28 co-stimulation in mouse and human T cells. J Exp Med. 2016;213:2437–57.
9. Karczewski KJ, Weisburd B, Thomas B, Solomonson M, Ruderfer DM, Kavanagh D, et al. The ExAC browser: displaying reference

data information from over 60 000 exomes. Nucleic Acids Res. 2017;45:D840–5.
10. Sherry ST, Ward MH, Kholodov M, Baker J, Phan L, Smigielski EM, et al. dbSNP: the NCBI database of genetic variation. Nucleic Acids Res. 2001;29:308–11.
11. The 1000 Genomes Project Consortium. An integrated map of genetic variation from 1,092 human genomes. Nature. 2012;491:56–65.
12. Scott EM, Halees A, Itan Y, Spencer EG, He Y, Abdellateef Azab M, et al. Characterization of greater middle eastern genetic variation for enhanced disease gene discovery. Nat Genet. 2016;48:1071–6.
13. Kumar P, Henikoff S, Ng PC. Predicting the effects of coding non-synonymous variants on protein function using the SIFT algorithm. Nat Protoc. 2009;4:1073–82.
14. Schwarz JM, Cooper DN, Schuelke M, Seelow D. Mutationtaster2: mutation prediction for the deep-sequencing age. Nat Methods. 2014;11:361–2.
15. Adzhubei IA, Schmidt S, Peshkin L, Ramensky VE, Gerasimova A, Bork P, et al. A method and server for predicting damaging missense mutations. Nat Methods. 2010;7:248–9.
16. Ashkenazy H, Abadi S, Martz E, Chay O, Mayrose I, Pupko T, et al. ConSurf 2016: an improved methodology to estimate and visualize evolutionary conservation in macromolecules. Nucleic Acids Res. 2016;44:W344–50.
17. Biasini M, Bienert S, Waterhouse A, Arnold K, Studer G, Schmidt T, et al. SWISS-MODEL: modelling protein tertiary and quaternary structure using evolutionary information. Nucleic Acids Res. 2014;42:1–7.
18. Zezos P, Patsiaoura K, Nakos A, Mpoumponaris A, Vassiliadis T, Giouleme O, et al. Severe eosinophilic infiltration in colonic biopsies predicts patients with ulcerative colitis not responding to medical therapy. Color Dis. 2014;16:O420–30.
19. Morgenstern S, Brook E, Rinawi F, Shamir R, Assa A. Tissue and peripheral eosinophilia as predictors for disease outcome in children with ulcerative colitis. Dig Liver Dis. 2017;49:170–4.
20. Bin Dhuban K, Piccirillo CA. The immunological and genetic basis of immune dysregulation, polyendocrinopathy, enteropathy, X-linked syndrome. Curr Opin Allergy Clin Immunol. 2015;15:525–32.
21. Posovszky C. Congenital intestinal diarrheal diseases: a diagnostic and therapeutic challenge. Best Pract Res Clin Gastroenterol. 2016;30:187–211.
22. Caudy AA, Reddy ST, Chatila T, Atkinson JP, Verbsky JW. CD25 deficiency causes an immune dysregulation, polyendocrinopathy, enteropathy, X-linked-like syndrome, and defective IL-10 expression from CD4 lymphocytes. J Allergy Clin Immunol. 2007;119:482–7.
23. Charbit-Henrion F, Jeverica AK, Bègue B, Markelj G, Parlato M, Avcin SL, et al. Deficiency in mucosa-associated lymphoid tissue lymphoma translocation 1: a novel cause of IPEX-like syndrome. J Pediatr Gastroenterol Nutr. 2017;64:378–84.
24. Uzel G, Sampaio EP, Lawrence MG, Hsu AP, Hackett M, Dorsey MJ, et al. Dominant gain-of-function STAT1 mutations in FOXP3 wild-type immune dysregulation-polyendocrinopathy-enteropathy-X-linked-like syndrome. J Allergy Clin Immunol. 2013;131:1611–1623.e3.
25. Kuehn HS, Ouyang W, Lo B, Deenick EK, Niemela JE, Avery DT, et al. Immune dysregulation in human subjects with heterozygous germline mutations in CTLA4. Science. 2013;4:6–11.
26. Alroqi FJ, Charbonnier LM, Keles S, Ghandour F, Mouawad P, Sabouneh R, et al. DOCK8 deficiency presenting as an IPEX-like disorder. J Clin Immunol. 2017;37:811–9.
27. Charbonnier LM, Janssen E, Chou J, Ohsumi TK, Keles S, Hsu JT, et al. Regulatory T-cell deficiency and immune dysregulation, polyendocrinopathy, enteropathy, X-linked-like disorder caused by loss-of-function mutations in LRBA. J Allergy Clin Immunol. 2015;135:217–27.
28. Liang Y, Cucchetti M, Roncagalli R, Yokosuka T, Malzac A, Bertosio E, et al. The lymphoid lineage–specific actin-uncapping protein Rltpr is essential for costimulation via CD28 and the development of regulatory T cells. Nat Immunol. 2013;14:858–66.
29. Matsushima N, Tachi N, Kuroki Y, Enkhbayar P, Osaki M, Kamiya M, et al. Structural analysis of leucine-rich-repeat variants in proteins associated with human diseases. Cell Mol Life Sci. 2005;62:2771–91.
30. Peters-Golden M, Henderson WR. Leukotrienes. N Engl J Med. 2007;357:1841–54.